



## BICRITICAL DYNAMICS OF PERIOD-DOUBLING SYSTEMS WITH UNIDIRECTIONAL COUPLING

A. P. KUZNETSOV, S. P. KUZNETSOV and I. R. SATAEV

*Institute of Radioengineering and Electronics, Academy of Sciences of the USSR, Saratov, USSR*

Received October 10, 1990; Revised April 16, 1991

The simplest case of bicritical behavior arises in a system of two logistic maps with unidirectional coupling in the point of a parameter plane where lines of transition to chaos in both subsystems meet. We develop a renormalization group analysis of the bicriticality and find the corresponding fixed point universal function and constants featuring the scaling properties of the second system while the first one is in the Feigenbaum critical state. Fractal properties of the bicritical attractor and its quantitative characteristics ( $\sigma$ -functions,  $f(\alpha)$ -spectra, generalized dimensions) are considered. It is shown that the bicriticality may be observed as well in lattice models of flow systems consisting of more than two coupled elements.

### 1. Introduction

One of the promising roads to understanding spatio-temporal chaos such as fluid turbulence consists in the construction and investigation of coupled map lattices recently introduced as simple but pithy models of spatially extended systems by several authors [Kaneko, 1984, 1985; Kuznetsov & Pikovsky, 1986; Crutchfield & Kaneko, 1987; Waller & Kapral, 1984; Aranson *et al.*, 1988]. Most of them are on lattices consisting of Feigenbaum period-doubling maps. Particularly, lattices with unidirectional coupling were proposed for the modeling of turbulence in flow systems [Kaneko, 1985; Aranson *et al.*, 1988]. Such lattices may also be easily constructed in electronics [Anishchenko *et al.*, 1986; Bezruchko *et al.*, 1986]. A number of phenomena have been discovered in systems of this class, among them are spatio-temporal chaos, spatial period doublings, saturation of attractor dimension down the flow, observations of the generation of moving domain walls by small random excitation and so on. Also, a new type of non-Feigenbaum critical behavior was found in an electronic system of two periodically excited nonlinear LC-circuits connected through a special amplifier securing the unidirectional character of coupling [Bezruchko *et al.*, 1986]. It is realized when

one simultaneously leads both subsystems just onto a border of chaos by their two control parameters. This point of parameter plane corresponds obviously to the onset of hyperchaos [Rössler, 1979]. It was called a *bicritical point* because of the natural analogy with phase transition theory. This usually denotes a point where two different lines of the second-order phase transitions meet.

The simplest model describing the bicriticality is a system of two logistic maps with unidirectional coupling:

$$x_{n+1} = 1 - \lambda x_n^2, \quad y_{n+1} = 1 - Ay_n^2 - Bx_n^2, \quad (1)$$

where  $x$  and  $y$  are dynamical variables of two coupled systems,  $\lambda$  and  $A$  are control parameters and  $B$  is a coupling constant.

In this work we present the renormalization group analysis of the bicriticality giving a foundation of quantitative universality for this situation, discuss the structure of parameter space and power spectra, consider the fractal structure of the bicritical attractor, introduce  $\sigma$ -functions,  $f(\alpha)$ -spectra and generalized dimensions describing scaling properties for bicriticality and show a possibility of its realization in more complicated lattice systems.

## 2. Renormalization Group Analysis

The ideas of the renormalization group (RG), universality and scaling appeared first in quantum field theory and phase transition theory. Beginning with Feigenbaum's works [Feigenbaum, 1979, 1980] they were introduced into the nonlinear system analyses and have promoted the better understanding of the dynamics at the onset of chaos through the period doubling sequence, intermittency and quasiperiodicity. Briefly, the contents of RG method is as follows. Given a dynamical system evolution operator over a definite time interval, one can build the evolution operator over somewhat greater time and then rescale the dynamical variables to make the resultant operator as similar to the initial one as possible. This is just RG transformation. It may be repeated to obtain the evolution operator over greater and greater times. It may then appear that, for certain values of control parameters for the considered dynamical system, the evolution operator becomes invariant under the RG transformation. In other words, it is a fixed point of RG transformation. It corresponds to some critical situation where universality and scaling are just valid. Universality is related to the fact that the operator is defined by the RG transformation structure rather than by the initial evolution operator. The existence of scaling is associated with the presence of greater-than-unity in-modulus eigenvalues of RG transformation linearized at the fixed point. Each of the eigenvalues is related to the essential parameter of the system and gives the scaling constant along the corresponding direction in the parameter space.

Let us apply the technique in the case of Eqs. (1).

Denoting the right sides in Eqs. (1) through  $g_0(x)$  and  $f_0(x, y)$ , perform the mapping twice and change the scales of  $x$  and  $y$  by some factors  $a$  and  $b$ . We then obtain

$$\begin{aligned} x_{n+2} &= ag_0(g_0(x_n/a)) , \\ y_{n+2} &= bf_0(g_0(x_n/a), f_0(x_n/a, y_n/b)) . \end{aligned} \tag{2}$$

The right hand functions we denote now as  $g_1(x)$  and  $f_1(x, y)$ . Repeating the procedure we come to recurrent RG equations

$$\begin{aligned} g_{m+1}(x) &= ag_m(g_m(x/a)) , \\ f_{m+1}(x, y) &= bf_m(g_m(x/a), f_m(x/a, y/b)) . \end{aligned} \tag{3}$$

The bicritical behavior must correspond to a fixed point of it:

$$g(x) = ag(g(x/a)) , f(x, y) = bf(g(x/a), f(x/a, y/b)) . \tag{4}$$

The functions  $g, f$  and factors  $a, b$  may be obtained by the solution of Eqs. (4). Under the normalization condition,  $g(0) = 1, f(0, 0) = 1$ , we have  $a = (g(1))^{-1}$  and  $b = (f(1, 1))^{-1}$ .

The first of Eqs. (4) is independent on the second one and its solution is a known Feigenbaum function  $g(x)$  with  $a = -2.502907$  [Feigenbaum, 1979, 1980]. The numerical solution of the second equation was undertaken by expansion of the unknown function  $f(x, y)$  through even Tchebyshev polynomials:

$$f(x, y) = \sum_m \sum_n C_{mn} T_{2m}(x) T_{2n}(y) , \quad x, y \in [-1, 1] . \tag{5}$$

Substituting it into Eqs. (4) and using the known polynomial representation of  $g(x)$  [Feigenbaum, 1979, 1980] we replace the functional equation by a set of  $M \times N$  nonlinear algebraic equations for  $C_{mn}$ . This procedure is based essentially on the property of orthogonality of Tchebyshev polynomials on a net formed in the  $(x, y)$ -plane by roots of the product  $T_{2M+1}(x)T_{2N+1}(y)$ . The solution was obtained by the Newton method. The values of  $M$  and  $N$  achieved in our calculations were 10 and 14. The polynomial approximation found for  $f(x, y)$  is presented in the Appendix with an accuracy up to the 6th digit and the plot of it is shown in Fig. 1a. The best evaluation of the scaling constant is  $b = 1.505318159$ .

The next step consists of investigating the evolution of small perturbations of the fixed point  $g(x), f(x, y)$  under RG transformation. We suppose that the perturbations do not violate the unidirectional nature of coupling. Under this condition there are two essential unstable directions of the fixed point. The first one corresponds to the perturbation removing the first system from the critical point and is associated with the known Feigenbaum's eigenfunction  $h(x)$  and eigenvalue  $\delta_1 = 4.66920$ . Another direction implies the perturbation of only the second subsystem:  $f_m(x, y) = f(x, y) + \delta^m \varphi(x, y)$  and leads to the eigenproblem

$$\begin{aligned} \delta \varphi(x, y) &= b[f'_x(g(x/a), f(x/a, y/b))\varphi(x/a, y/b) \\ &+ \varphi(g(x/a), f(x/a, y/b))] . \end{aligned} \tag{6}$$

Using the above representation of function (5) we have solved it by straightforward iterations and found the eigenfunction  $\varphi(x, y)$  (Fig. 1b) and eigenvalue

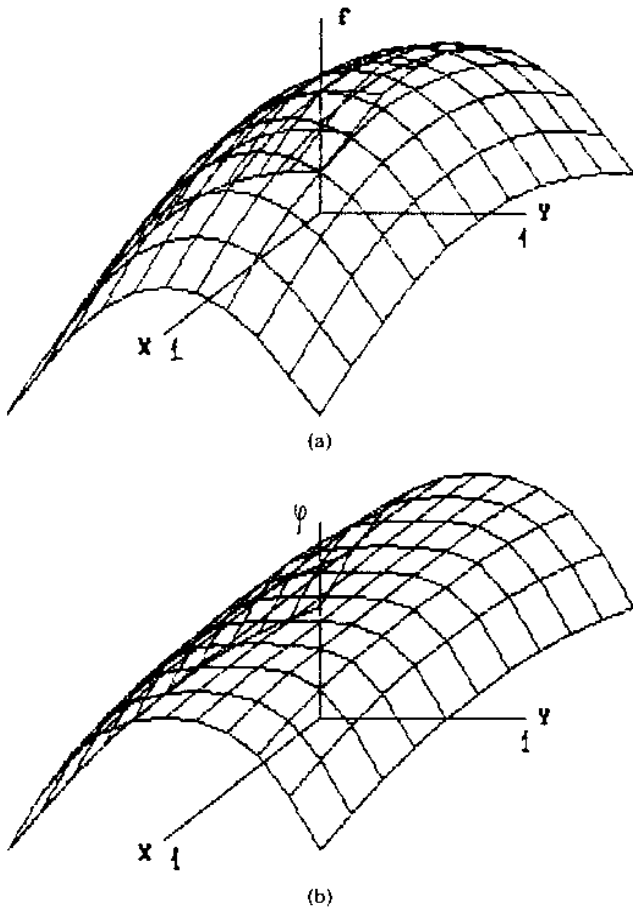


Fig. 1. Plots of the universal functions  $f(x, y)$  and  $\varphi(x, y)$  found by solution of the RG equations (4) and (6).

$\delta_2 = 2.39272443$ . We point out that new constants  $b$  and  $\delta_2$  are in good agreement with earlier empirical evaluation of scaling factors ( $b \approx -1.51$ ,  $\delta_2 \approx 2.39$ ) [Bezruchko *et al.*, 1986].

The map

$$x_{n+1} = g(x_n), \quad y_{n+1} = f(x_n, y_n),$$

describing the long time dynamics exactly in the bicritical situation has a fixed point  $x_* = 0.54931$ ,  $y_* = 0.52807$ . Then it follows evidently from RG equations (4) that a period-2 cycle exists, one of elements being  $x_*/a$ ,  $y_*/b$ . It means, furthermore, the existence of a period-4 cycle with the elements  $x_*/a^2$ ,  $y_*/b^2$  and so on *ad infinitum*. All these cycles are unstable and have the same multipliers found to be equal  $\mu_x = g'(x_*) = -1.60119$  and  $\mu_y = f'_y(x_*, y_*) = -1.17886$ .

The last property is useful for the exact calculation of bicritical points for the model map (1). In the first system we take  $\lambda = \lambda_c = 1.401155$  for  $g_m$  going to  $g$ .

Then we find, by Newton's method, the cycles of (1) with periods  $2^k$  and  $\mu_k = \prod_{i=1}^{2^k} (-2Ay_i)$  and select a value of  $A = A_c$  to make  $\mu_k$  equal to the universal constant  $-1.17886$  for sufficiently large  $k$ . So  $(\lambda_c, A_c)$  will just be the bicritical point. In Fig. 2a the calculated dependence of multipliers  $\mu_k$  on  $A$  and  $k$  is shown for  $B = 0.375$ . One can see an expected intersection of all multipliers with large  $k$  in the bicritical point. From calculations we find, in this case,  $A_c = 1.124981403$ . Figure 2b shows  $A_c$  versus  $B$ .

Notice, that the system under consideration has, in general, a lot of attractors. Indeed, in the case of  $B = 0$

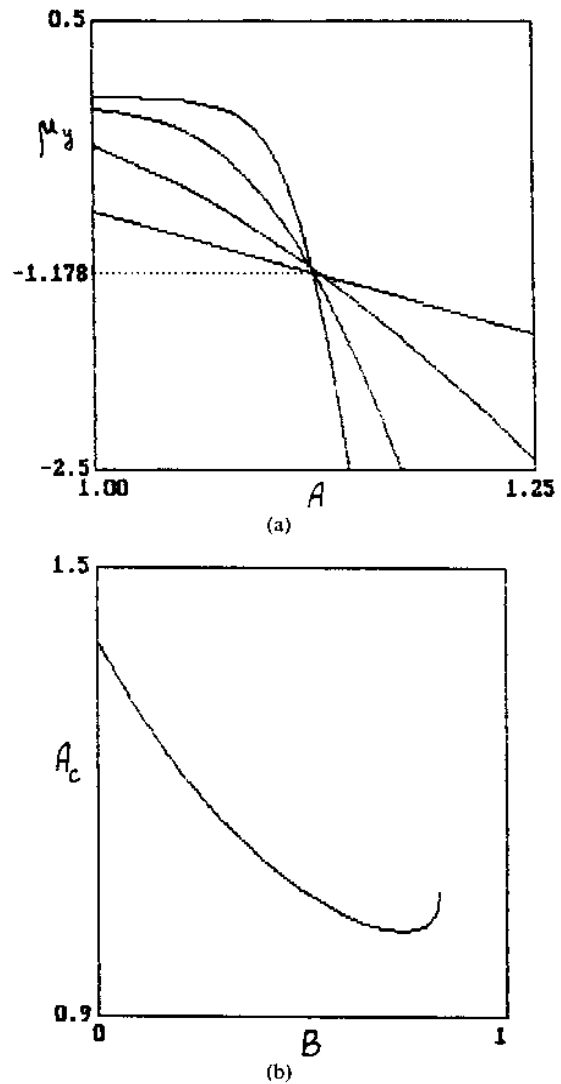


Fig. 2. The multiplier  $\mu_y$  of period-2, 4, 8, 16 cycles versus  $A$  for  $\lambda = \lambda_c = 1.4011552$  and  $B = 0.375$  (a) and the bicritical line in the  $(A, B)$ -plane (b).

it breaks up into the two uncoupled period-doubling systems. If they both have stable  $2^k$ -cycles then the composed system has  $2^k$  stable states distinguished by the phase shift between subsystems. Multistability is preserved after coupling, at least while its value is small enough. In this report we discuss in detail one of the attractors whose basin include the point  $x = y = 0$ . Bicritical situation may be found for other attractors too, the scaling constants being the same. It is an effective demonstration of the bicritical dynamics universality which is proved in the framework of the RG approach.

In conclusion, we must emphasize that the presence of bicriticality is strongly connected with the unidirectional character of coupling. It may be shown that the introduction of contradirectional interaction destroys the bicriticality because of newly appearing unstable directions of the RG fixed point.

### 3. Scaling Properties of Parameter Space Near the Bicritical Point

Consider two points of parameter space  $\lambda = \lambda_c + \Delta\lambda$ ,  $A = A_c + \Delta A$  and  $\lambda = \lambda_c + \Delta\lambda/\delta_1$ ,  $A = A_c + \Delta A/\delta_2$  with the same  $B$ 's. It is obvious that  $\Delta\lambda$  contributes only to the perturbation of the RG fixed point associated with Feigenbaum's eigenfunction  $h(x)$  and eigenvalue  $\delta_1$  and that  $\Delta A$  contributes only to the perturbation corresponding to the eigenfunction  $\phi(x, y)$  with eigenvalue  $\delta_2$ . So the iterations of the RG transformation (3) in two considered points will accordingly lead to the same map after  $m$  and  $m + 1$  iterations. Thus, the dynamical regimes in these points will be similar with characteristic time doubling in the second case.

In Fig. 3 the structure of the  $(\lambda, A)$ -plane is shown for  $B = 0.375$ . In the vicinity of the bicritical point, there is a complicated configuration of regions including periodical regimes (clear zones), chaotic regimes with one of the Lyapunov exponents

$$\Lambda_x = \lim \frac{1}{N} \sum_{i=1}^N \ln |2\lambda x_i|, \quad \Lambda_y = \lim \frac{1}{N} \sum_{i=1}^N \ln |2A y_i|, \quad (7)$$

positive (horizontal and vertical dashes) and hyperchaos with  $\Lambda_x, \Lambda_y > 0$  (doubled dashes). For the system with unidirectional coupling the presence of hyperchaos is tested easily since each Lyapunov exponent associates with definite subsystem [Aranson *et al.*, 1988].

For evidence of scaling one may compare three pictures (Figs. 4a, b, c) showing the region of  $\Lambda_y > 0$ . In

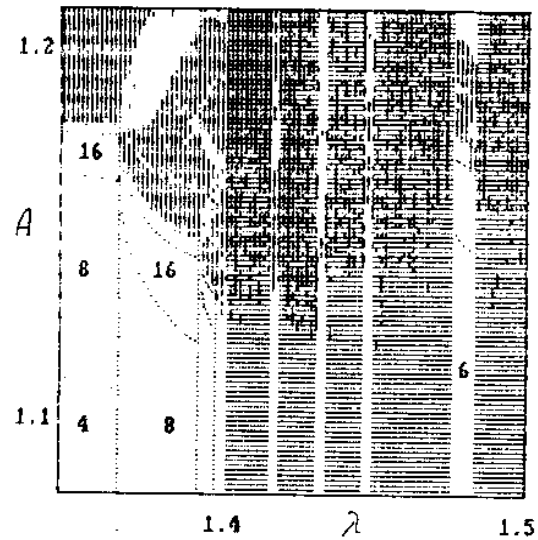


Fig. 3. Configuration of dynamical regimes in the  $(\lambda, A)$ -plane for  $B = 0.375$ . Clear zones correspond to periodic states, and the numbers are for cycle periods. Horizontal dashes correspond to chaos in the first subsystem only, vertical — chaos in the second subsystem, doubled dashes — hyperchaos.

Figs. 4b, c the picture is presented under onefold and twofold magnification by factor  $\delta_1$  for the  $\lambda$ -axis and  $\delta_2$  for the  $A$ -axis. One can see that each successive picture reproduces the previous one with an accuracy increasing with the depth of resolution.

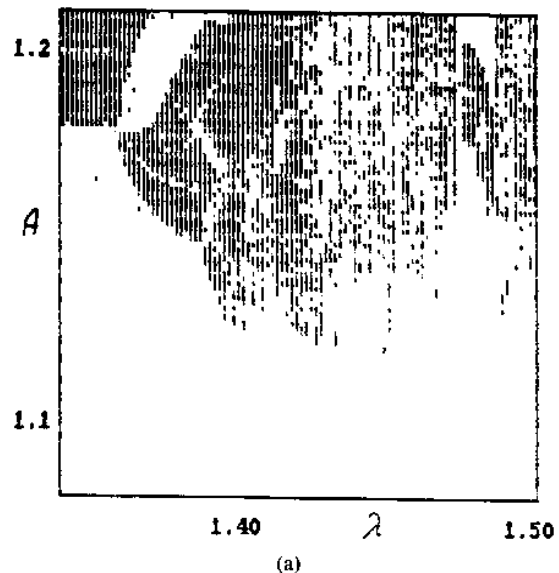
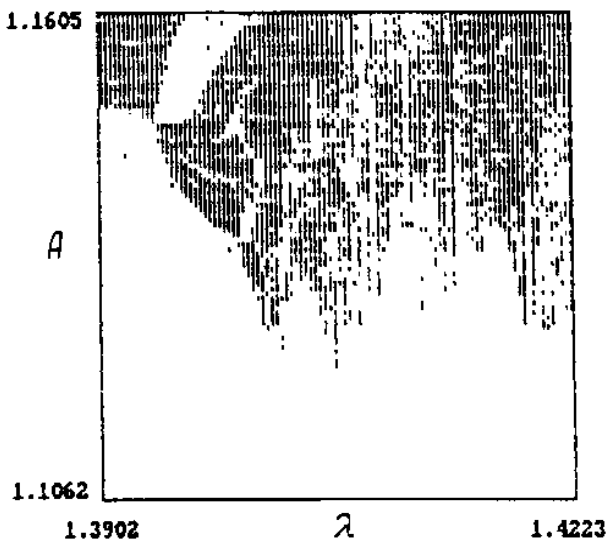
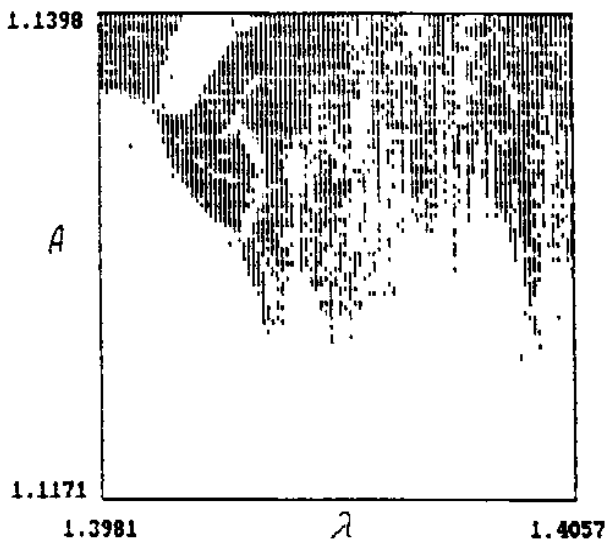


Fig. 4. Regions of positive Lyapunov exponent  $\Lambda_y$  of the second system at different scales: the magnification from one picture to the next is determined by the factor  $\delta_1$  along the  $\lambda$ -axis and by  $\delta_2$  along the  $A$ -axis.



(b)



(c)

Fig. 4. (Continued).

Let us consider in more detail how the dynamics is changed when we move upward in the parameter plane along the line  $\lambda = \lambda_c$  through the bicritical point. The plot of Lyapunov exponent  $\Lambda_y$  versus the parameter  $A$  is shown in Fig. 5a. The Lyapunov exponent is negative for  $A < A_c$  and becomes positive for  $A > A_c$  excluding some windows of regularity. So the bicritical point is really a border of chaos in the second system when the first one is in the critical state. Also, the bifurcation tree is presented in Fig. 5b. This is the plot of  $y$ 's running during long time dynamics of the map

(1) (after the exception of transients) versus the parameter  $A$ . Already for  $A < A_c$ , each branch of the bifurcation tree has a fine structure reproducing the structure of Feigenbaum's attractor. It is caused by forcing the second system with the first one and can be seen under suitable magnification. An evolution of this structure when  $A$  goes to  $A_c$  is smooth. Exactly in the point  $A_c$  a set with new fractal properties is formed which we shall discuss further.

Scaling properties of the Lyapunov exponent and bifurcation tree are illustrated by a comparison of the initial pictures of Figs. 5a, b with its magnified parts shown in Figs. 5c, d, e, f. The change of scale along the  $A$ -axis is determined by the factor  $\delta_2 = 2.39272$ , for the  $A$ -axis it is equal to 2 and for the  $y$ -axis to  $b = 1.50532$ .

So we really observe the expected scaling near the bicritical point, and can now turn to a discussion of the dynamics exactly in this point.

#### 4. Bicritical Attractor

We shall see now that the attractor in the bicritical point is a very interesting example of a multifractal set in a two-dimensional phase space  $(x, y)$ . To understand its geometric nature we recall the known procedure for constructing Feigenbaum's attractor. Given  $x_0 = 0$  one iterates the map  $x_{n+1} = 1 - \lambda_c x_n^2$  and obtains a sequence  $x_1, x_2, x_3, \dots$ . Then the 0th level of the construction is a segment  $[x_1, x_2]$ , the 1st level is a unification of two segments  $[x_1, x_3]$  and  $[x_2, x_4]$ , the 2nd level is a unification of four segments  $[x_1, x_5]$ ,  $[x_2, x_6]$ ,  $[x_3, x_7]$ ,  $[x_4, x_8]$  and so on. Each set obtained at some step of the construction contains all the successive sets in itself. So the limit object is just Feigenbaum's attractor.

To construct the bicritical attractor, we begin from the initial point  $x_0 = 0, y_0 = 0$  and find a sequence of pairs  $(x_1, y_1), (x_2, y_2), (x_3, y_3), \dots$  by iterations of Eqs. (1). The 0th level of the construction will be a rectangle with opposite vertices in  $(x_1, y_1)$  and  $(x_2, y_2)$ . We denote it as

$$\Pi_0 = \{(x_1, y_1), (x_2, y_2)\} .$$

The 1st level will be presented by two rectangles with opposite vertices in  $(x_1, y_1), (x_3, y_3)$  and  $(x_2, y_2), (x_4, y_4)$ :

$$\Pi_1 = \{(x_1, y_1), (x_3, y_3)\} \cup \{(x_2, y_2), (x_4, y_4)\} .$$

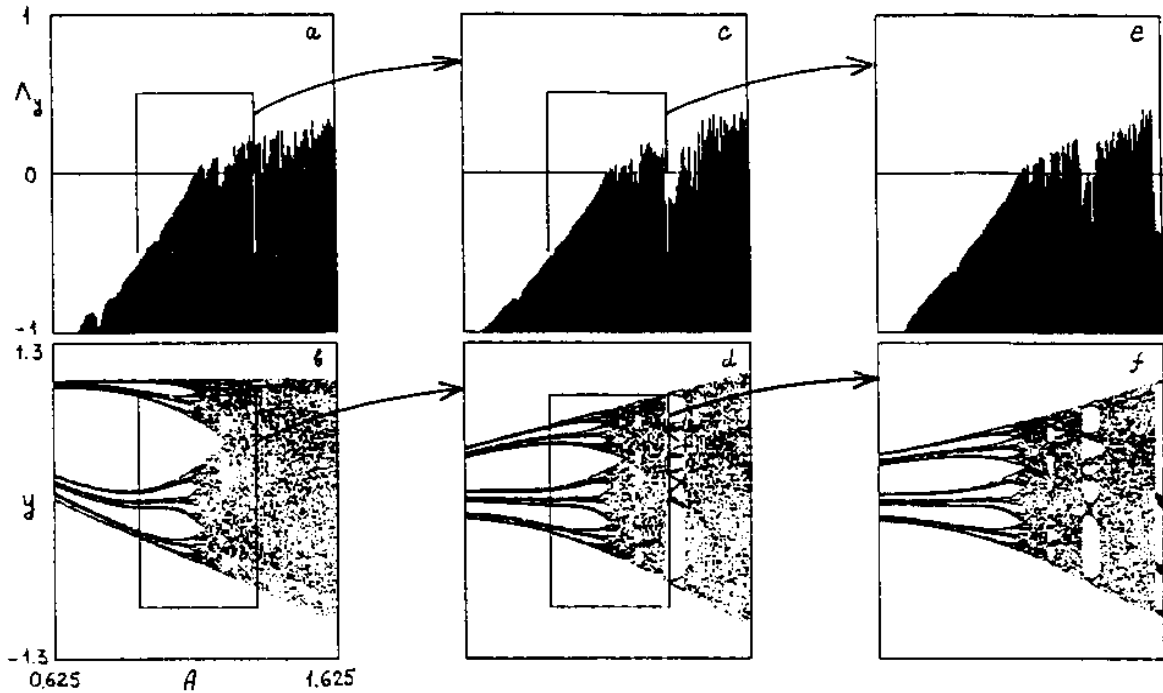


Fig. 5. Lyapunov exponent  $\Lambda_y$  versus  $A$  and bifurcation trees  $y$  versus  $A$  for  $\lambda = \lambda_c = 1.4011552$ ,  $B = 0.375$ . The next pictures present the magnified parts of the previous ones inside the rectangles shown. For the best evidence of scaling only the points for each 2nd and 4th temporal steps are shown at (d) and (f).

Then we continue the construction shown in Fig. 6. On the  $n$ th level we have

$$\Pi_n = \bigcup_{i=1}^{2^n} [(x_i, y_i), (x_{i+2^n}, y_{i+2^n})], \quad (8)$$

giving the bicritical attractor in the limit of  $n \rightarrow \infty$ .

Let us evaluate now the Hausdorff dimension of this set. At the  $n$ th level of construction it is approximated by  $2^n$  rectangles of size  $l_i \times L_i$ . For large  $n$  these rectangles stretch along the  $y$ -axis and so  $L_i \gg l_i$  (see Fig. 6 and further discussions of  $\sigma_x$  and  $\sigma_y$  functions). A number of squares of size  $l_i$  needed for covering the rectangle is given by  $L_i/l_i$ . Following the traditional definition of the Hausdorff dimension. [Farmer, 1982], we consider a sum of  $l_i^D$  over all squares and rectangles:

$$S_n = \sum_{i=1}^{2^n} (L_i/l_i) \cdot l_i^D,$$

and choose the value of  $D$  to provide for  $S_n$  to be finite in the limit of  $n \rightarrow \infty$ . Then  $D$  will be the Hausdorff dimension of the set. By numerical calculations we find  $D \approx 1.0794$ .

For global characterization of scaling properties of the bicritical attractor, we introduce two functions

$\sigma_x$  and  $\sigma_y$  according to Feigenbaum's proposition [Feigenbaum, 1979, 1980]:

$$\begin{aligned} \sigma_x(m/2N) &= \frac{x'_m - x'_{m+N}}{x_m - x_{m+N/2}}, \\ \sigma_y(m/2N) &= \frac{y'_m - y'_{m+N}}{y_m - y_{m+N/2}}, \end{aligned} \quad (9)$$

where  $m, N = 2^n \rightarrow \infty$ ,  $x_m, y_m$  and  $x'_m, y'_m$  are the elements of the period- $N$  and  $-2N$  cycles of the map (1) in the bicritical point. These functions, as numerically calculated, are shown in Fig. 7. Because of the independence of the dynamics of the first system on the second one, the function  $\sigma_x$  is just the known Feigenbaum function. On the contrary,  $\sigma_y$  is a new universal function for scaling properties of the  $y$ -projection of the bicritical attractor. The fact that  $|\sigma_y| > |\sigma_x|$  infers that the splitting distance of trajectories along the  $y$ -axis decreases more slowly than along the  $x$ -axis under an increase of resolution of the attractor structure.  $\sigma_y$  as well as  $\sigma_x$  has discontinuities in all binary rational points of  $m/2^n$ . We note that this fine structure is more noticeable for  $\sigma_y$  than for  $\sigma_x$ .

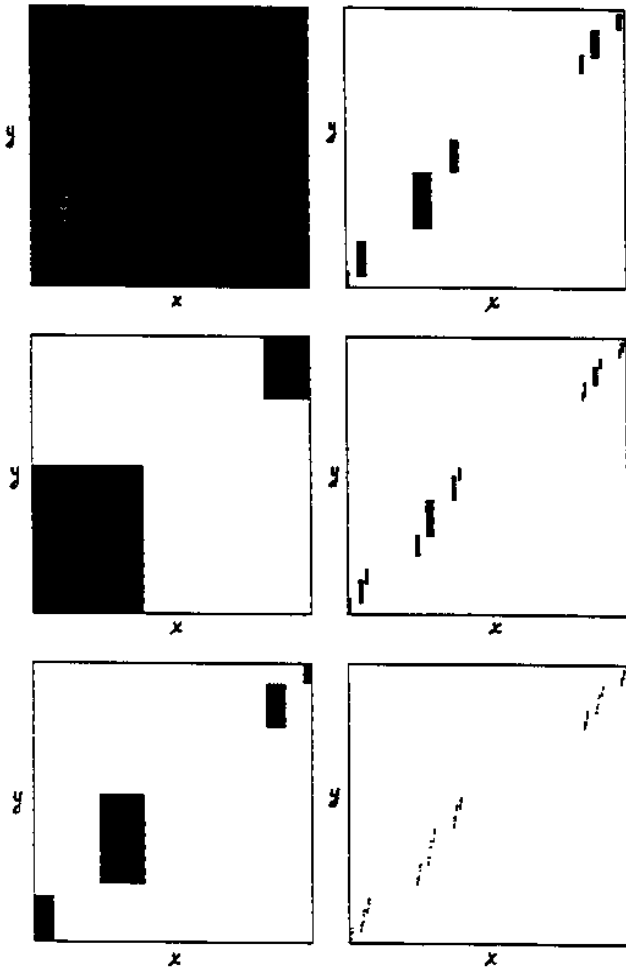


Fig. 6. Construction of a bicritical attractor in the  $(x, y)$  plane,  $B = 0.375$ .

It is known that these relations exist for Feigenbaum's attractor:

$$\sigma_x(+0) \rightarrow 1/a^2, \quad \sigma_x(1/2-0) \rightarrow 1/|a|, \quad (10)$$

$$a = -2.50291.$$

For  $\sigma_y$  we find, similarly,

$$\sigma_y(+0) \rightarrow 1/b^2, \quad \sigma_y(1/2-0) \rightarrow 1/|b|, \quad (11)$$

$$b = -1.50532.$$

Roughly one can represent  $\sigma_x$  and  $\sigma_y$  by two steps of levels (10) and (11). It corresponds to an approximation of the attractor by an object whose projections onto the coordinate axes are two-scale Cantor sets [Halsey *et al.*, 1986] with scale parameters  $1/a$ ,  $1/a^2$  and  $1/b$ ,  $1/b^2$ . For Feigenbaum's attractor this approximation leads to useful relations for the power spectrum, dimensions,  $f(\alpha)$ -spectrum and so on. A simple

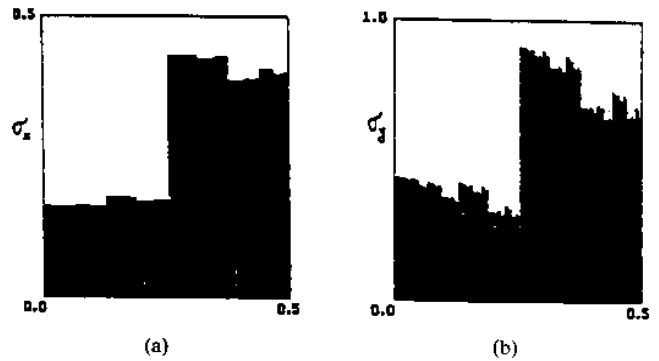


Fig. 7. Plots of the functions  $\sigma_x$  and  $\sigma_y$ , which determine the global scaling properties of the  $x$ - and  $y$ -projections of the bicritical attractor.

generalization of it for the  $y$ -projection of the attractor will be discussed further.

In Fig. 8 the numerically calculated power spectra of  $x$  and  $y$  variables in the bicritical point are shown. The first one is an ordinary Feigenbaum's spectrum. The second one is a specific bicritical spectrum characterized by non-Feigenbaum relations between subharmonics of distinguishable levels. Using the above two-scale approximation with scaling factors (11) one obtains the next recurrent relation for spectral intensities of  $y$ :

$$\frac{1 + b^2 \pm 2b \cos(\pi\omega/2)}{4b^4} S(\omega) \rightarrow \begin{cases} S(\omega/2), & \text{sign "-"}, \\ S(1-\omega/2), & \text{sign "+"}, \end{cases} \quad (12)$$

analogous to the known result for the Feigenbaum spectrum [Huberman & Zisook, 1981; Nauenberg & Rudnik, 1981] with  $a$  changed to  $b$ . We find that (12)

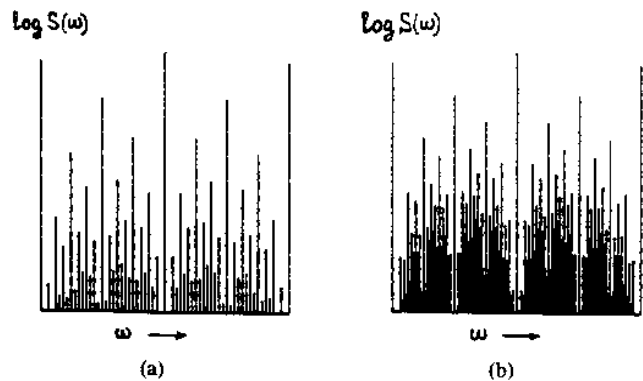


Fig. 8. Power spectra generated at bicritical point by the first (a) and by the second (b) subsystem.

is in good agreement with Fig. 8b and gives the mean difference between neighboring levels

$$\Delta S = 10 \log(1/4b^2 + 1/4b^4) \approx -8.0 \text{ dB} .$$

This value is essentially smaller than the level difference in Feigenbaum's spectrum which is -13.4 dB. So the high order subharmonics are higher in level in the  $y$ -spectrum in comparison with the  $x$ -spectrum.

Let us now turn to the evaluation of the spectrum of scaling indices  $f(\alpha)$ . We shall support, here, a view that this spectrum is an attribute of a signal generated by a "black box" rather than a characteristic of the bicritical attractor. We have two signals,  $x_n$  and  $y_n$ , and confine ourselves, here, by its independent processing. Using the same procedure as proposed earlier for the Feigenbaum case [Halsey et al., 1986] we define the partition function at the  $n$ th level of resolution

$$\Gamma_n = \sum_{i=1}^{2^n} p_i^q / l_i^\tau , \tag{13}$$

where  $p_i = 1/2^n$ ,  $l_i = |x_i - x_{i+2^n}|$  or  $|y_i - y_{i+2^n}|$ ,  $x_i, y_i$  are sequences generated by (1) at the bicritical point with initial condition  $x_0, y_0 = 0$ . Then we demand that  $\Gamma_n$  be finite for  $n \rightarrow \infty$ :

$$q = \frac{1}{n} \log_2 \left| \sum_{i=1}^{2^n} l_i^{-\tau} \right| . \tag{14}$$

Following [Halsey et al., 1986] we obtain the  $f(\alpha)$ -spectrum in parametric form

$$\alpha = \frac{d\tau}{dq}, \quad f = \alpha q - \tau . \tag{15}$$

In two-scale approximation, the sum  $\Gamma_{n+1}$  may be obtained from  $\Gamma_n$  by changing each term  $p^q/l^\tau$  by two terms:

$$\frac{|a|^\tau p^q}{2^q l^\tau} + \frac{|a|^{2\tau} p^q}{2^q l^\tau} \text{ for } x \text{ and}$$

$$\frac{|b|^\tau p^q}{2^q l^\tau} + \frac{|b|^{2\tau} p^q}{2^q l^\tau} \text{ for } y .$$

So we have  $\Gamma_{n+1} = (|a|^\tau + |a|^{2\tau}) 2^{-q} \Gamma_n$  for  $x$  and  $\Gamma_{n+1} = (|b|^\tau + |b|^{2\tau}) 2^{-q} \Gamma_n$  for  $y$ . Then we obtain, accordingly,  $q = \log_2(|a|^\tau + |a|^{2\tau})$  and  $q = \log_2(|b|^\tau + |b|^{2\tau})$ , and find  $\alpha$  and  $f$  from (15) analytically.

Figure 9 shows the  $f(\alpha)$ -spectra generated both by  $x$  and  $y$ . Dotted lines indicate two scale approximation while solid lines show accurate numerical calculations. For the first variable  $x$  we have, of course, a traditional Feigenbaum's form [Halsey et al., 1986], but the second spectrum is specific. It is disposed on an interval of  $\alpha$ 's from  $1/\log_2 b^2 = 0.84736$  to  $1/\log_2 |b| = 1.69472$  and has an extremum at  $f = D_0^{(y)} \approx 1.1714$ . We call this value the fractal dimension of the signal  $y$ .

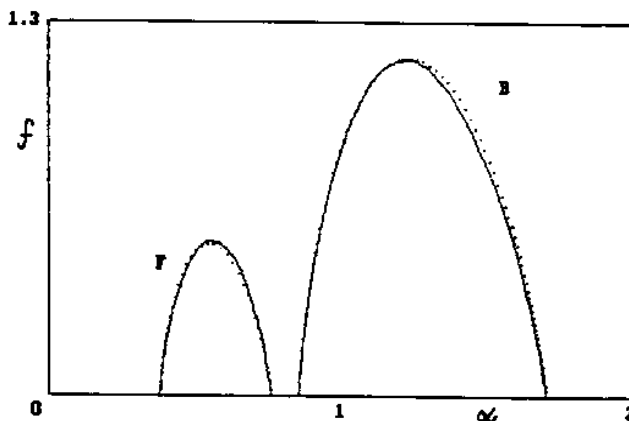


Fig. 9. Plots of  $f(\alpha)$ -spectra generated by both subsystems in the bicritical point. The spectrum for the first system is denoted by F ("Feigenbaum"), the second one by B ("bicritical").

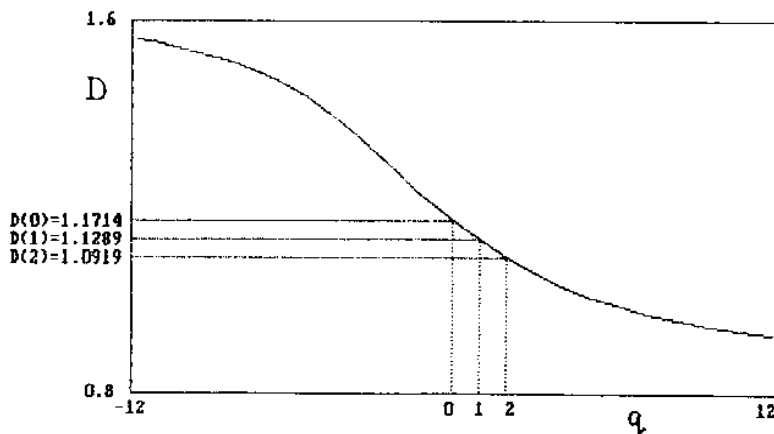


Fig. 10. The generalized dimension  $D(q)$  of signal  $y$  at the bicritical point.



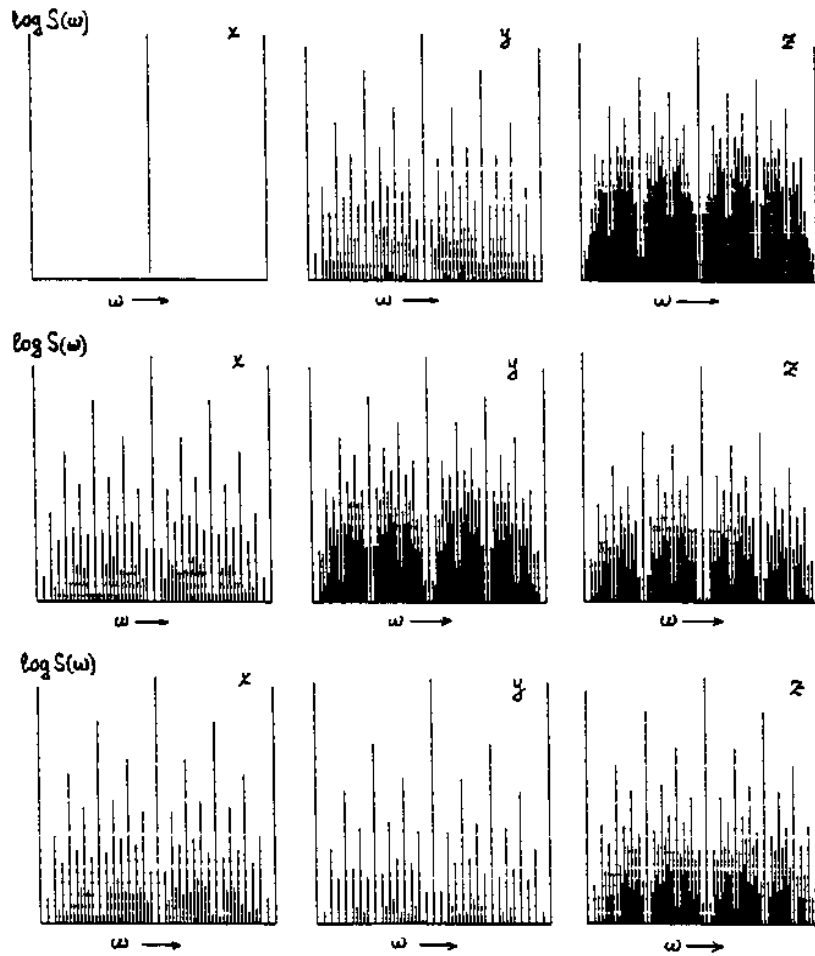


Fig. 11. Power spectra generated by the three systems with unidirectional coupling Eq. (16) in different situations realizing the bicriticality (see text): a)  $\lambda = 1, A = 1.272008, B = 0.25, C = 1.128102, D = 0.375$ ; b)  $\lambda = 1.401155, A = 1.124981, B = 0.375, C = 0.6, D = 0.375$ ; c)  $\lambda = 1.401155, A = 0.8, B = 0.375, C = 1.179791, D = 0.375$ .

One could expect that this is the Hausdorff dimension of the  $y$ -projection of the bicritical attractor. However this is not true because of the interweaving of  $y$ -projections of different elements for the construction of the set (see Fig. 6). It is connected also with the fact that  $D_0^{(y)} > 1$ . In spite of it the value  $D_0^{(y)}$  may be considered as some kind of dimension reflecting scaling properties of  $y$ 's. With similar reservations, we may define the whole set of generalized dimensions  $D_q^{(y)} = \tau/(1 - q)$  [Halsey *et al.*, 1986]. The plot of them is shown in Fig. 10, where some important particular cases are pointed out by corresponding numerical values.

### 5. Lattices of Three and More Elements

The bicriticality is a widely spread universal type of behavior of flow systems when two or more control

parameters are taken into account. One can meet it not only in the system of two coupled elements. For example in a system of three elements

$$\begin{aligned} x_{n+1} &= 1 - \lambda x_n^2, & y_{n+1} &= 1 - Ay_n^2 - Bx_n^2, \\ z_{n+1} &= 1 - Cz_n^2 - Dy_n^2, \end{aligned} \tag{16}$$

we can secure the next bicritical situations:

1. By taking  $\lambda < \lambda_c$  for the first system, which would demonstrate some stable cycle, and selecting  $A$  to realize the Feigenbaum's critical situation in the second system, and  $C$  to obtain bicriticality in the third system. This situation may be represented by the diagram

$$P \rightarrow F \rightarrow B,$$

where  $P$  denotes the periodic behavior,  $F$  — the

Feigenbaum's critical dynamics, and  $B$  — the bicritical dynamics;

- By taking  $\lambda = \lambda_c$  and  $A = A_c$  for given  $B$  and not large  $C$  and  $D$ . Then the second system will be in the bicritical state while the third one accomplishes the forced movement with scaling properties intrinsic to bicriticality:

$$F \rightarrow B \rightarrow B ;$$

- For  $\lambda = \lambda_c$  and not large  $A$  and  $B$ , we have the Feigenbaum critical state in the first system and an induced state with the same scaling properties in the second one. So, by suitable selection of  $C$  for given  $D$  one can obtain the bicriticality in the third system:

$$F \rightarrow F \rightarrow B .$$

Figure 11 presents the power spectra of subsystems in these three situations. Comparing them with standard Feigenbaum and bicritical spectra (Fig. 8) supports the listed diagrams. The number of possible variants becomes greater with increasing number of lattice elements. For instance the states

$$P \rightarrow P \rightarrow F \rightarrow B, \quad F \rightarrow F \rightarrow F \rightarrow B,$$

$$P \rightarrow F \rightarrow F \rightarrow B, \quad F \rightarrow F \rightarrow B \rightarrow B,$$

$$P \rightarrow F \rightarrow B \rightarrow B, \quad F \rightarrow B \rightarrow B \rightarrow B,$$

may be realized in the lattice of 4 elements and so on.

## References

- Anischenko, V. S., Aranson, I. S., Postnov, D. E., Rabinovich, M. I. [1986] "Spatial synchronization and bifurcation of the chaos development in a chain of connected generators," *Dokl. Akad. Nauk USSR* **286**, pp. 1120–1124.
- Aranson, I. S., Gaponov-Grekhov, A. V., Rabinovich, M. I. [1988] "The onset and spatial development of turbulence in flow systems," *Physica* **D33**, pp. 1–20.
- Bezruchko, B. P., Gulyaev, Yu. V., Kuznetsov, S. P., Seleznev, E. P. [1986] "New type of critical behavior in coupled systems at the transition to chaos," *Dokl. Akad. Nauk USSR* **287**, pp. 619–622.
- Crutchfield, J. P. & Kaneko, K. [1987] "Phenomenology of spatio-temporal chaos," in *Directions in Chaos*, ed. Hao B.-L. (World Scientific, Singapore) pp. 272–353.
- Farmer, J. D. [1982] "Chaotic attractors of an infinite dimensional dynamical systems," *Physica* **D4**, pp. 366–393.
- Feigenbaum, M. J. [1979] "The universal metric properties of nonlinear transformations," *J. Stat. Phys.* **21**, pp. 669–706.
- Feigenbaum, M. J. [1980] "The transition to aperiodic behavior in turbulent systems," *Comm. Math. Phys.* **77**, pp. 65–86.
- Halsey, T. S., Jensen, M. H., Kadanoff, L. P., Procaccia, I., Shraiman, B. I. [1986] "Fractal measures and their singularities," *Phys. Rev.* **A33**, pp. 1141–1151.
- Huberman, B. & Zisook, A. [1981] "Power spectra of strange attractors," *Phys. Rev. Lett.* **26**, pp. 626–632.
- Kaneko, K. [1984] "Period doubling of kink-antikink patterns, quasiperiodicity in antiferrolike structures in coupled logistic lattice," *Prog. Theor. Phys.* **72**, pp. 480–486.
- Kaneko, K. [1985] "Spatial period-doubling in open flow," *Phys. Lett.* **A111**, pp. 321–325.
- Kuznetsov, S. P. & Pikovsky, A. S. [1986] "Universality and scaling of period-doubling bifurcations in a dissipative distributed medium," *Physica* **D19**, pp. 384–396.
- Nauenberg, M. & Rudnik, J. [1981] "Universality and the power spectrum at the onset of chaos," *Phys. Rev.* **B24**, pp. 493–495.
- Rössler, O. E. [1979] "An equation for hyperchaos," *Phys. Lett.* **A71**, pp. 155–157.
- Waller, I. & Kapral, R. [1984] "Spatial and temporal structure in systems of coupled nonlinear oscillators," *Phys. Rev.* **A30**, pp. 2047–2055.

## Appendix

We present here the polynomial approximation of the function  $f(x, y)$  found by numerical solution of RG-equations (4) with precision up to the 6th digit:

$$\begin{aligned}
 f(x, y) = & 1 - 0.8555209y^2 - 0.4327171y^4 + 0.0884042y^6 + 0.1685034y^8 - 0.0111849y^{10} + 0.0397315y^{12} \\
 & - 0.1233151y^{14} + 0.0863301y^{16} - 0.0246471y^{18} + 0.0024956y^{20} + x^2[-0.5969284 - 0.3038808y^2 \\
 & + 0.0919502y^4 + 0.1862281y^6 - 0.0217993y^8 + 0.068305y^{10} - 0.2391765y^{12} + 0.1939734y^{14} \\
 & - 0.0641303y^{16} + 0.0076191y^{18}] + x^4[-0.0318577 + 0.0570438y^2 + 0.085061y^4 - 0.0180487y^6 \\
 & + 0.0402246y^8 - 0.1979341y^{10} + 0.1952681y^{12} - 0.0764447y^{14} + 0.0107490y^{16}] + x^6[0.0175115 \\
 & + 0.0184702y^2 - 0.0091169y^4 + 0.0094340y^6 - 0.0920556y^8 + 0.1171801y^{10} - 0.0557729y^{12} \\
 & + 0.0093699y^{14}] + x^8[0.0009261 - 0.0029286y^2 - 0.0001536y^4 - 0.0254408y^6 + 0.0456733y^8 \\
 & - 0.0273932y^{10} + 0.0055839y^{12}] + x^{10}[-0.0004461 - 0.0004062y^2 - 0.0038934y^4 + 0.0116841y^6 \\
 & - 0.0093343y^8 + 0.0023675y^{10}] + x^{12}[-0.0000111 - 0.0002252y^2 + 0.0018605y^4 - 0.0021846y^6 \\
 & + 0.0007198y^8] + x^{14}[-0.0000065 + 0.0001533y^2 - 0.0003310y^4 + 0.0001534y^6] + x^{16}[0.0000061 \\
 & - 0.0000270y^2 + 0.0000212y^4] + x^{18}[-0.0000003 + 0.0000015y^2] ,
 \end{aligned}$$